AFRL-AFOSR-UK-TR-2021-0017

Plasma Driven Hypersonic Testing

Bland, Simon
IMPERIAL COLLEGE OF SCIENCE TECHNOLOGY & MEDICINE
EXHIBITION RD
LONDON, ,
GB

06/24/2021
Final Technical Report

Air Force Research Laboratory
Air Force Office of Scientific Research
European Office of Aerospace Research and Development
Unit 4515 Box 14, APO AE 09421

REPORT DOCUMENTATION PAGE

Form Approved
OMB No. 0704-0188

1. REPORT DATE *(DD-MM-YYYY)*	**2. REPORT TYPE**	**3. DATES COVERED** *(From - To)*
24-06-2021	Final	15 Dec 2016 - 14 Mar 2021

4. TITLE AND SUBTITLE
Plasma Driven Hypersonic Testing

5a. CONTRACT NUMBER

5b. GRANT NUMBER
FA9550-17-1-0036

5c. PROGRAM ELEMENT NUMBER

6. AUTHOR(S)
Simon Bland

5d. PROJECT NUMBER

5e. TASK NUMBER

5f. WORK UNIT NUMBER

7. PERFORMING ORGANIZATION NAME(S) AND ADDRESS(ES)
IMPERIAL COLLEGE OF SCIENCE TECHNOLOGY & MEDICINE
EXHIBITION RD
LONDON,
GB

8. PERFORMING ORGANIZATION REPORT NUMBER

9. SPONSORING/MONITORING AGENCY NAME(S) AND ADDRESS(ES)
EOARD
UNIT 4515
APO AE 09421-4515

10. SPONSOR/MONITOR'S ACRONYM(S)
AFRL/AFOSR IOE

11. SPONSOR/MONITOR'S REPORT NUMBER(S)
AFRL-AFOSR-UK-TR-2021-0017

12. DISTRIBUTION/AVAILABILITY STATEMENT
A Distribution Unlimited: PB Public Release

13. SUPPLEMENTARY NOTES

14. ABSTRACT
This report details initial experiments exploring the use of pulsed power driven dense plasma flows for hypersonics research. Such flows have regularly been produced for laboratory scale astrophysics studies, however, detailed characteristics of the flows and their interactions with different targets placed in the flow have rarely been studied for hydrodynamics purposes.

15. SUBJECT TERMS

16. SECURITY CLASSIFICATION OF:			**17. LIMITATION OF ABSTRACT**	**18. NUMBER OF PAGES**	**19a. NAME OF RESPONSIBLE PERSON**
a. REPORT	**b. ABSTRACT**	**c. THIS PAGE**			JASON FOLEY
U	U	U	SAR	33	**19b. TELEPHONE NUMBER** *(Include area code)* 555-555-5555

TABLE OF CONTENTS

LIST OF FIGURES

ACKNOWLEDGEMENTS

The research described in this report was carried out by the MAGPIE team at Imperial College, in particular Dr Eleanor Tubman (who was directly paid by the funding), Dr Lee Suttle, Dr Jack Halliday, Dr Jack Hare, Dr Tom Clayson, Danny Russell, Stefano Merlini and Vicente Valenzuela Villaseca.

1.0 EXECUTIVE SUMMARY

This report details initial experiments exploring the use of pulsed power driven dense plasma flows for hypersonics research. Such flows have regularly been produced for laboratory scale astrophysics studies, however, detailed characteristics of the flows and their interactions with different targets placed in the flow have rarely been studied for hydrodynamics purposes.

The experiments were all performed on the ~2MA MAGPIE (Mega-Ampere-Generator-for-Plasma-Implosion-Experiments) pulsed power facility at Imperial College and leveraged a set of cutting edge diagnostics including high speed optical emission imaging, laser interferometry, schlieren photography, multi-point Thomson scattering, Faraday rotation imaging and XUV imaging. The experiments were performed in 3 different configurations: utilizing plasma generated by an inverse (aka 'exploding') cylindrical wire array z-pinch; utilizing the plasma jet generated above an ablating foil placed between radially concentric electrodes; and finally utilizing the flow of plasma from the surface of a solid target being ablated by an intense X-ray pulse.

Plasma flowing from an inverse wire array ~20mm diameter was found to have a velocity of ~50kms^{-1}. Electron densities in the flow were ~1x10^{18}cm^{-3}, and the electron and ion temperatures between 10 and 20eV. The plasma flow had a sonic Mach number of ~2.5 (and in some configurations up to 5), however it was discovered that the plasma flow included an entrained magnetic field of 4-5T limiting the effective Mach number in the flow. The entrained field strongly affected interactions between the flow and test targets, depending on the targets conductivity, orientation and size. Providing the target was smaller than the magnetic diffusion length in the flow (~1mm), or the target was insulating there was little affect of the entrained magnetic field on the formation of shocks around the target – i.e. the flow was effectively hydrodynamic in nature, and the shock characteristics that of a hypersonic flow. However, if a conducting target was used that was larger than the diffusion length, the entrained field could pile up in front of the target producing an artificially wide shock separated from the target. In order to attempt to remove this limitation on target design methods to remove the entrained field were explored. A grid of copper wires reduced the magnetic field downstream of the grid by a factor of ~5, resulting in bow shocks formed close to test targets – however the field could not be completely eliminated.

In an attempt to create a flow of plasma without an entrained magnetic field, a solid metallic foil was used in between radially concentric electrodes, 6mm and 40mm in diameter. Above the central electrode, ablation of the foil produces a dense jet of similar diameter to the central electrode. The electron density in the jet was measured to be ~1x10^{19} cm^{-3}, its temperature ~ 10-20eV and the velocity at which it propagated was ~100kms^{-1} – giving a sonic Mach number in this flow > 5. Faraday rotation measurements suggested that minimal magnetic field was present in the jet. A small spherical target placed in the jet resulted in a well-defined single bow shock at the target, consistent with simple hydrodynamic theory. A rod placed along the axis of the jet showed a single bow shock at its tip, and multiple subsequent shocks along the length of the rod. This could be due to a radiative cooling instability developing at the bow shock or the development of Kelvin-Helmholtz instability in the boundary layer at the rod surface. However the diameter of the jet did limit the size of objects that could be explored.

Finally attempts were made to create a large (cm) scale flow of dense, hypersonic plasma by using X-ray driven ablation of a solid target. To achieve this an imploding wire array z-pinch was used

to produce a TW burst of soft X-ray radiation over ~25ns. Solid silicon targets were placed ~20mm from the pinch, and plasma observed to expand from their surface over 100s of ns. The electron density, speed and temperature of the plasma flow was similar to our previous experiments at $1x10^{19}$ cm^{-3}, ~50kms^{-1} and ~10-20eV; crucially though in this case the plasma was not created with an entrained magnetic field. The Mach number in the flow was ~4, and our first experiments interacting the plasma flow with wedge targets generated shock waves that were again consistent with simple hydrodynamic theory. This new method of radiatively driven ablation, could potentially become the hypersonics testing platform we aimed to create in the project.

2.0 INTRODUCTION

Vehicles capable of travelling at hypersonic speed offer huge benefits for military and civil applications, yet their behavior is extremely difficult to model, necessitating the use of complex 3D hydrodynamics codes operating at multiple scales. In order to provide validation of the codes and perform tests of models across different scales, hypersonic wind tunnels are regularly employed. These typically store large volumes of gas at very high pressures that is then fed (via a burst diaphragm) through a specifically shaped nozzle to generate hypersonic flow. The design of such tunnels has not changed greatly over the last few decades – and a modern hypersonic wind tunnel might produce a flow of a few kms^{-1} (Mach 5-10) have an nozzle diameter 10s of cm in scale and maintain flows of 10s of ms. This is perfect for a huge amount of aeronautical/hydrodynamic tests, but the cost and scale of modern hypersonic wind tunnel facilities can make access difficult – potentially restricted research and limiting the ability of the field to attract new talent.

The use of dense plasma flows, created through the pulsed power ablation and acceleration of wires and/or foils could provide a new, complimentary route for studying hypersonic affects. Such flows can be produced on 10ns – 1000ns time scales, cm length scales and rapidly attain velocities of 10s – 100s of kms^{-1}. The largest use of these flows to date has been to explore dynamic astrophysical processes in the laboratory, and a number of cutting-edge diagnostics have been developed to help provide detailed characteristics of the plasmas. Further, the pulsed power technology used to ablate the materials is undergoing a renaissance, with compact, modern systems capable of producing Mega-Ampere currents in table top sized devices. However, prior to dense plasma flows finding use as a test bed for hypersonic studies, there are a number of key questions that need answering, in particular what effects could magnetic fields that are potentially entrained in the plasma flow as it is created have on subsequent interactions between the plasma flow and a target, and can these affects be mitigated if they are found to be important.

2.1 Dense plasma flows created from the pulsed power driven ablation of wires

The dense plasma flows created in pulsed power experiments typically have Reynolds numbers of $\sim 10^6 - 10^7$, as such they could be expected to obey the same Euler scaling laws as an inviscid fluid, however their behavior is complicated by the presence of both electrons and ions, and with this the ability of a plasma to be affected by electric and magnetic fields. For the purpose of this research, magnetic fields in the plasma flow could strongly alter their interaction with any targets, and so we will concentrate discussions around the effects associated with these – basically the difference between a purely hydrodynamic flow and a 'magneto-hydrodynamic' flow.

An important parameter that helps quantify the behavior of magnetic fields in a plasma is the 'magnetic Reynolds number', R_M. This is a measurement of the advection of the magnetic field with the flow of a plasma, scaled to the diffusion of the field through the flow. A $R_M << 1$ typically represents movement of the field through a very poorly conducting plasma, with the magnetic field free to diffuse through it; whilst a $R_M >> 1$ represents an ideal conducting plasma with field 'frozen in the flow'. An expression for R_M is:

$$R_M = \mu_0 svL \qquad [1]$$

where σ is the conductivity of the plasma, v is the velocity of the plasma flow and L is the scale length. Typically the warm, dense plasmas created through pulsed power driven ablation of wires and foils have R_M ~ 10-100, hence it is likely that at least some of the magnetic field created by the high currents flowing through the wires will become entrained in this ablated plasma flow. The effects of this field will depend on whether it can advect with the plasma flow past the target or diffuse through a target. If the target is relatively small, field embedded in the plasma could simply move past the target, and the interactions between the target and flow become hydrodynamic in nature. If however the target is relatively large then magnetic field can pile up at the interaction between the target and flow, subsequently altering the flow – for example bow shocks can become significantly detached from their targets and shockwaves in the flow widened. Even if the target itself is insulating – which should enable magnetic field to diffuse through a target – the volume of plasma at the boundary between a large target and the plasma flow could result in the magnetic field increasing here, and this field dominating the flow dynamics, as the plasma itself is a conductor.

Whether or not a flow can be considered as purely hydrodynamic is also reflected in the Mach number we can use to describe the flow. In a plasma the 'sonic' Mach number is given by:

$$\mathrm{M_S} = \frac{\text{velocity of plasma flow}}{\text{ion sound speed}} \quad [2]$$

$$\textit{where the ion sound speed} = \left(\frac{\gamma Z T_e}{m_i}\right)^{\frac{1}{2}} \quad [3]$$

this is equivalent to the usual speed of sound used in aeronautics. However, in the presence of a magnetic field, information can be passed at a much greater speed through the plasma as magnetic waves – this is the Alfvén speed. A separate Mach number, the Alfvén Mach number, can then be defined as:

$$\mathrm{M_A} = \frac{\text{velocity of plasma flow}}{\text{Alfvén wave speed}} \quad [4]$$

$$\text{where Alfvén wave speed} = \frac{\mathrm{B}}{\sqrt{\mu \mathrm{n_i} \mathrm{m_i}}} \quad [5]$$

The two Mach numbers can be combined into a new metric, the magnetosonic Mach number through:

$$\mathrm{M_{MS}} = \left(\frac{1}{\mathrm{M_S}^2} + \frac{1}{\mathrm{M_A}^2}\right)^{-1/2} \quad [6]$$

Interacting a flow with simple test targets enables the flows Mach number to be readily estimated. A small spherical object placed into a supersonic flow will generate a bow shock close to the surface of the object, the opening angle of which (measured far away from the interaction point) is given by:

$$\sin \mu = \frac{1}{M} \quad [7]$$

Hence in an experiment, if the Mach number measured from the opening angle of a bow shock matches the sonic Mach number calculated from measurements of the flow speed and ion sound speed then the flow is behaving purely hydrodynamically, and the effects of any magnetic field are minimal. However if the Mach speed measured from a bow shock is much lower than the sonic Mach number, magnetic fields may be important in the flow. Similarly, a wedge placed into a superonic flow will produce an oblique shock, that can be related back Mach number of the flow by the β- θ-M relation:

$$\tan\vartheta = 2\cot\beta \frac{M^2\sin^2\beta - 1}{M^2(\gamma + \cos 2\beta) + 2} \quad [8]$$

where θ is the angle of the wedge and β the angle of the shock, both with respect to the flow

In a purely hydrodynamic flow, hypersonic research is classified as when the Mach speed is > 5; in the case of plasmas with entrained fields, M_{MS} should be >5 for the flow to be in this regime.

2.2 Aims of the project

The overarching aim of the project was to determine whether dense plasma flows created utilizing pulsed power could be used to make a platform for hypersonic research. As such the project was divided into 5 tasks:

i) Characterization of the plasma flow from an inverse array.
ii) Performing simple hydrodynamics/hypersonics experiments in the plasma flows.
iii) To look at methods of reducing any entrained magnetic field in a flow / use alternate experimental configurations.
iv) Explore the if we could diagnose target material ablated into the flow.
v) To explore more complex hypersonic interactions e.g. the formation of shocks between 2 hypersonic flows and the generation of Kelvin-Helmholtz instabilities in a flow.

3.0 METHODS TO MAKE A HYPERSONIC PLASMA FLOW

3.1 Plasma flow from an inverse array

Inverse wire array z-pinches [1] consist of a central conductor surrounded by a cylindrical arrangement of fine metallic wires. Current travelling through the wires returns via the central conductor. Rather than homogeneously exploding over the entire volume of the wire (and all of this material being instantly converted into plasma) ohmic heating at the wires forms a 2 part 'core-corona' structure with cold, relatively dense wire 'cores' acting as reservoirs for warm lower density plasma that ablates from their surface over 100s of ns. Current flowing through this corona plasma interacts with the induced magnetic field from the central conductor via the $\mathbf{J} \wedge \mathbf{B}$ force, resulting in a flow of the plasma into a force free region around the wires (fig.1).

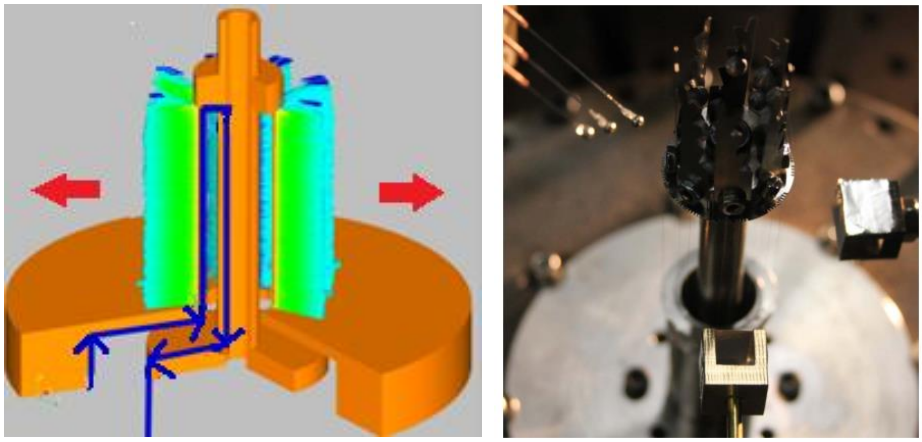

Fig.1 Left: schematic showing current flow through wires of an inverse array (blue) and plasma flows into force free region around array. Right: experimental set up for test experiments showing inverse array and target objects

Our previous research has indicated that whilst the majority of the current remains close to the wire cores, acting on the plasma just as it ablates, some of the current (and hence azimuthal magnetic field) becomes entrained in the plasma flow. In order to understand how this might affect interactions between the plasma flow and targets, the first set of experiments completed for the project utilized small diameter cylindrical targets placed parallel and perpendicular to expected direction of the field in the flow– as shown in fig. 2.

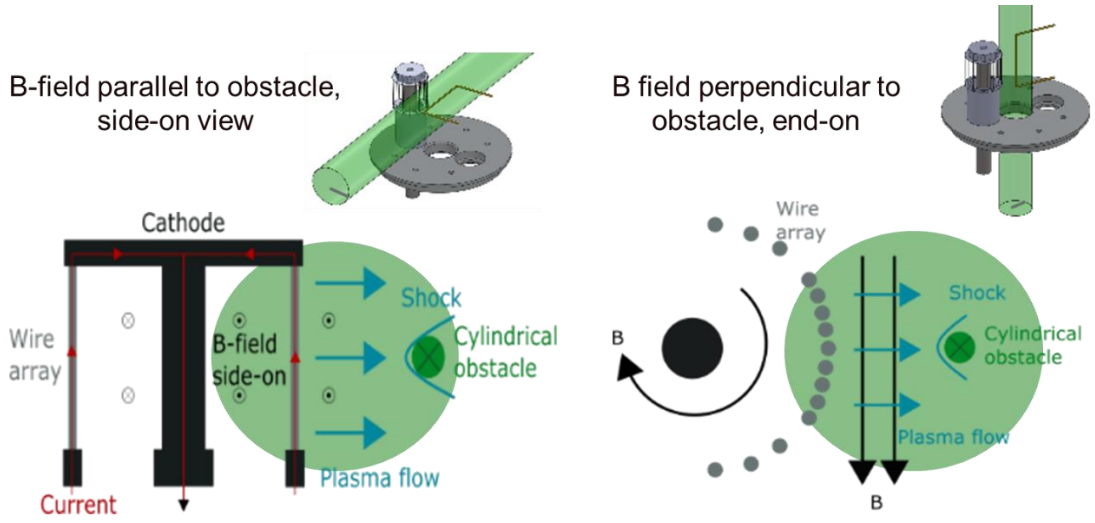

Fig.2 Left: schematic showing dense plasma flow from wires and target parallel to magnetic field in the flow. The green cylinder represents the line of site of the probing laser. Right: schematic with target perpendicular to field. Note in both cases wires are bunched on 1 side of the array to produce a more uniform flow of plasma

The experiments were performed on the MAGPIE pulsed power facility at Imperial college with currents of 1.4MA peak and rise times ~240ns long [2]. The diameter of the inverse array was 16mm, and aluminum or copper wires were utilized to make the plasma flow. Targets were 0.5mm brass cylinders several cm in length placed 1-2cm from the circumference of the array. The experiments were analyzed with an assortment of cutting edge optical and X-ray diagnostics [3] [4]. A high speed optical emission camera recorded 12 frames, each 5ns duration with variable interframe time (usually 20ns). A 4 frame XUV camera recorded soft X-ray emission (>30eV) on similar timescales. A Nd-YAG laser supplied ~0.3nm long pulses @ 1064nm and 532nm to interferometry and schlieren imaging channels, enabling the electron density of the plasma to be determined along with the geometry of any shock waves in the flow. A Thompson scattering system was utilized across multiple points in the plasma enabling the plasma velocity, T_e and ZT_i to be determined. Interferometry data constrained this measurements allowing Z and T_i to be found separately. A 1053nm Faraday imaging diagnostic measured rotation in the polarization of the probing beam, yielding direct information on the field in the plasma flow. Finally current through the entire experiment, and sometimes that induced in the target, were monitored using Rogowski grooves.

Experiments with a 0.5mm quartz cylinders in place of the brass cylinders enabled the diffusion of the magnetic field through a target to be explored. Finally, we performed experiments with much larger (4mm) cylindrical quartz targets parallel to the magnetic field to determine how the scale length of the interaction region between the flow and the target could affect how the magnetic field was advected here with the flow, and the subsequent affects on dynamics.

3.1.1 Stripping magnetic field from the plasma flow of an inverse array

Over the course of our research it became clear that in order for interaction of the plasma flow with the target to be unaffected by the magnetic field in the flow, the target had to be relatively small, and preferably non-metallic (including any support). This would place significant

restrictions on the use of different target geometries, so methods to strip the entrained field in the plasma flow were explored. One way to accomplish this introduced a grid of 50μm copper wires perpendicular to the azimuthal field. At each wire bow shocks form and the magnetic field density increases, but the plasma continues to flow through the grid reducing the field in the downstream flow – as shown in fig 3.

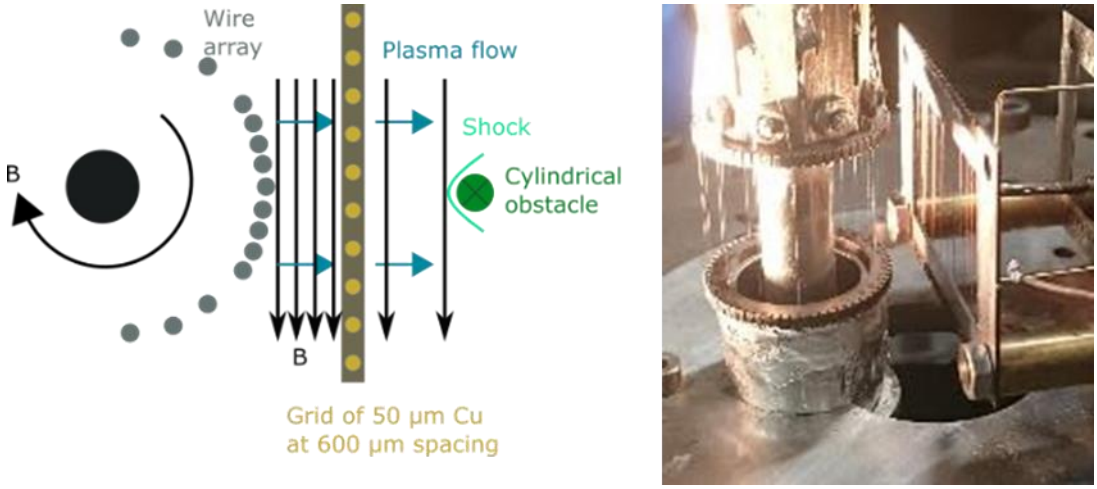

Fig.3 Left: schematic showing use of grid to attempt to reduce field in plasma flowing from inverse array. Right: Image showing grid in experiment

3.2 Use of the jet from a radial foil

During the project it became clear that the entrained magnetic field in the dense plasma flowing from an inverse wire array would be difficult to remove completely from the flow, limiting the viability of its use as a hypersonics platform. Hence we explored difference experimental configurations. The first of these was based on the radial foil z-pinch, that had also been used previously for scaled astrophysics experiments [5].

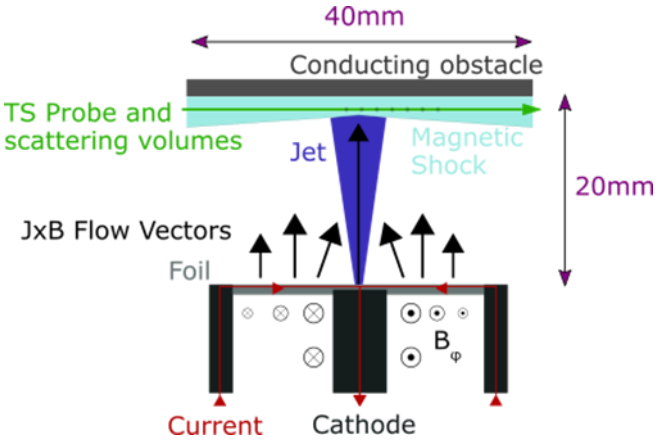

Fig.4 A schematic of the radial foil set-up for the MAGPIE generator. The jet is produced by plasma flow being deflected to the central axis and propagates outwards from the foil. Obstacles placed into the flows, can be planar (as depicted) or can be protruding into the jet as a rod or spherical object, creating bow shocks at their surfaces.

A schematic of the experimental set-up is shown in fig. 4. Current flows radially along a radial 14um thick Al foil stretched between the cathode rod of 6.35mm diameter and the coaxial 40mm diameter return conductor. This current path produces an azimuthal magnetic field below the foil reaching a peak of ~90T at the time of current maximum. Diffusion of a fraction of the current (and of magnetic field) through the resistively heated foil leads to generation of a plasma at the top surface of the foil which is accelerated by the $\mathbf{J} \wedge \mathbf{B}$ force in the direction approximately normal to the foil surface, creating a supersonic plasma outflow. Due to the relatively large foil thickness used in these experiments the foil itself remains essentially stationary for the entire duration of the experiment, while the outflow formed by continuously ablated plasma is sustained for 100s of ns. Above the cathode rod radial expansion of the plasma flowing from the foil produces a dense plasma jet. Due to the cylindrical symmetry of the outflow the advected magnetic field must be zero at the jet axis and we might expect that in the region above the cathode it remains relatively low.

Targets including ~0.5mm diameter spheres, were placed into the jet to explore their interaction with the plasma flow. These spheres were supported from the side of the jet. Long brass rods 0.5mm in diameter were placed end on into the flow of the jet. In order to support these a thick metal disk was introduced 2-4cm above the surface of the foil. This did not affect the dynamics of the jet close to the surface of the foil, though plasma could readily be observed piling up on the disk.

3.3 Use of radiation driven ablation to make hypersonic plasma flow

Whilst radial foil z-pinches enabled us to explore interactions between dense non-magnetized plasma flows and a target, the diameter of the plasma jet in these experiments limited the size of usable targets to the mm scale. Hence we investigated a further method to make dense plasma flows, through use of soft X-ray radiation to ablate a solid material. The outflow of ablated material was then used as the plasma flow for interaction experiments. By decoupling the ablation process from the current drive we hoped that this system would enable the creation of a plasma flow from the silicon without the entrainment of a magnetic field into this flow due to the ohmic heating that would otherwise drive ablation.

To generate soft X-ray radiation the Mega-ampere current pulse generated by MAGPIE was directed through an imploding wire array z-pinch [6]. Such imploding z-pinches are highly efficient sources of radiation, with research in the 1990s-2000s demonstrating ~300TW class X-ray pulses at National facilities [7]. Previous experiments on MAGPIE produced soft X-ray bursts over ~30ns with ~15KJ yields and radiation temperatures ~150eV. For these experiments cm^2 silicon targets were placed ~5-10 cm from the axis of the pinch and the intensity of radiation at the target was estimated as ~$10GW/cm^2$. Being so close to the pinch the targets were subject to the a few tesla azimuthal magnetic field generated by the current flowing through the pinch, however we used a geometry in which the azimuthal magnetic field lines were oriented parallel to the outflow from the target in order to mitigate these effects. In future experiments shielding or increasing the distance between the target(s) and the pinch and/or timing could completely exclude magnetic fields from any interaction experiment without significant modifying the conditions of the plasma outflow.

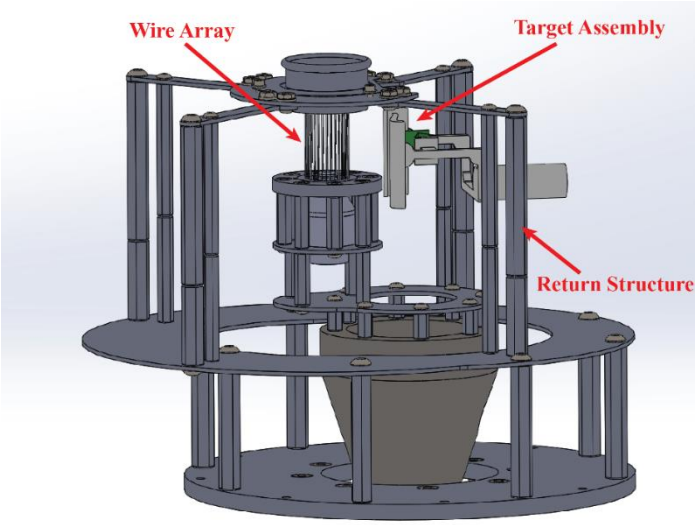

Fig.5 A CAD model showing an imploding wire array Z-pinch and a target assembly. During an experiment, the wire array produces X-Rays which irradiate the target, driving a plasma outflow.

Fig. 5 shows the design of the experiments utilizing an imploding wire array z-pinch and a silicon ablator The silicon is placed in the assembly shown in fig. 6. This consists of a plastic 3D printed shell/shade that supports the Si and a glass obstacle that acts as the target for the outflowing plasma from the silicon. The glass obstacle is shielded from the driving radiation by a plastic.

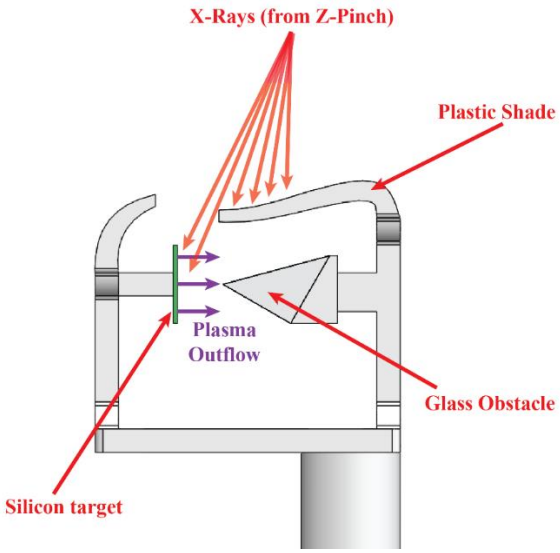

Fig.6 A top-down view of a target assembly which was used for a radiatively driven experiment. The image shows a silicon ablation target (from where plasma was launched), and a glass obstacle (with which the plasma flow collides). Arrows indicate the X-Ray flux cast from the Z-pinch onto the silicon ablator. A plastic shield was employed to prevent the direct irradiation of the glass obstacle by the driving radiation.

4.0 RESULTS AND DISCUSSION

4.1 Results from inverse array experiments

Thomson scattering and interferometry measurements of the plasma flow from an aluminium inverse wire array gave $n_e \sim 10^{18}$ cm^{-3}; the velocity of the flow to be ~50kms^{-1} and $T_e \sim T_i$ ~10-20eV. With these parameters the ion sound speed is ~ 21kms^{-1}, hence the sonic Mach number is ~2.5. The magnetic Reynolds number of the flow was estimated to be ~1-10. As expected from such a plasma, experiments with the cylindrical brass targets confirmed that magnetic field was entrained into the flow from the array affecting the interaction between the flow and targets.

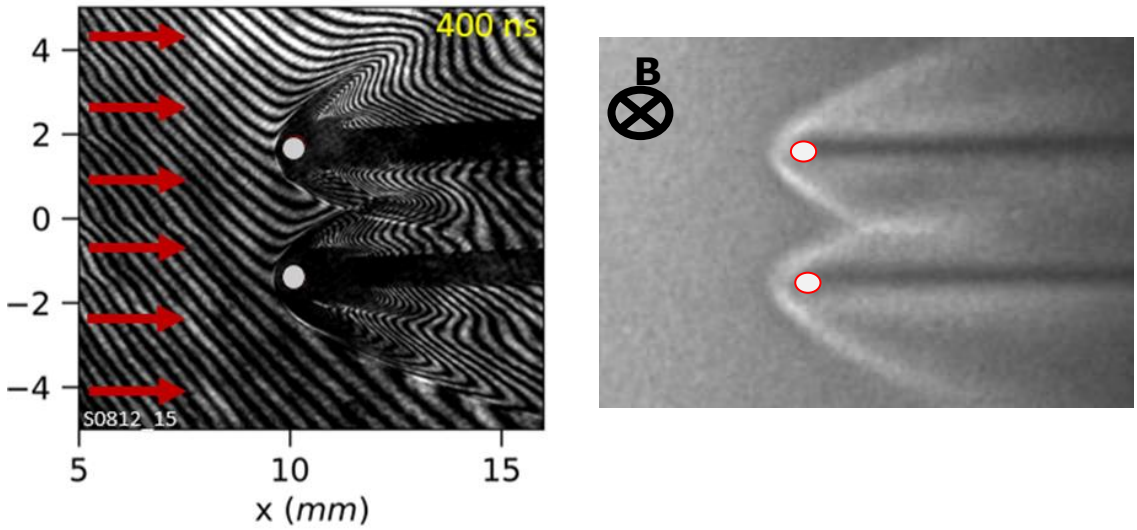

Fig 7. Left: interferogram of two 0.5mm diameter cylindrical brass targets in the flow of plasma produced from an inverse wire array (to the left, out of image). Bow shocks form close to the targets. field in plasma flowing from inverse array. Right: High speed self emission image of experiment, again show bow shocks forming close to each target, along with interaction of the shockwaves between the targets.

With the targets placed parallel to the azimuthal magnetic field expected in the flow, bow shocks were observed to form close to the surface of the targets, as can be seen in Fig 7. Far from interaction point, the shockwave has an angle of ~25^0 to the flow, which would suggest a Mach speed of 2.3. This consistent with the sonic Mach number calculated for the flow. However, if the orientation of the target(s) is now changed to be perpendicular to the field, the bow shocks become significantly separated from the targets by 1-2mm and the opening angle of the shockwave increases to ~45^0, as seen in Fig. 8.

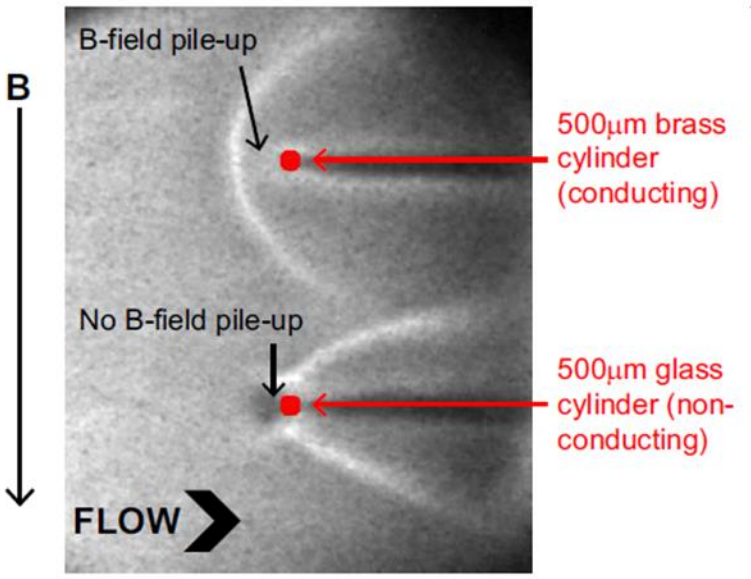

Fig. 8. Optical emission image of two 0.5mm diameter cylindrical targets placed in the flow from an inverse wire array z-pinch. The targets are both several cm long (into the page) and arranged perpendicular to the magnetic field expected in the flow. The upper target is made of brass, the lower quartz.

The behavior of the two brass targets follows on from the expectation of magnetic field being entrained in the plasma flow. Each target had a relatively small diameter ~0.5mm, which was comparable to the scale length over which diffusion and advection in the flow are equal. Hence for the target placed parallel to the azimuthal field lines in fig. 7, field could for the most part flow past the target and the flow after the target was dominated by hydrodynamic effects. When the length of the cylinder was aligned perpendicular to the direction of the field in fig 8, this could not happen. Instead field would be expected to 'pile up' at the boundary of the brass target with he flow, as eddy currents in the target would resist any diffusion of the field through the target. The increased magnetic field density separates the bow shock from the target and increases the opening angle of the bow shock.

One way that this effect can be negated is through the use of insulating targets. As seen in the lower part of the emission image in fig. 8, with a 0.5mm diameter quartz cylinder replacing the brass cylinder, the bow shock once again formed at the boundary of the target and the plasma flow; further the opening angle of the shock wave then match that seen in experiments with the brass cylinders placed parallel to the magnetic field in the flow (as in fig. 7). This is consistent with field being able to diffuse through the insulating target rather than piling up at the boundary.

However, simply restricting further experiments to using just insulating targets would omit potential issues with the size of the target which can also play a key factor in the interactions flow and any entrained field. To illustrate this with two 4mm quartz cylinders, separated by ~9mm (centre to centre) were placed in the plasma flow from an inverse array, again with their length aligned along the direction of the magnetic field expected in the flow. An interferogram of the experiment is shown in Fig. 9, below.

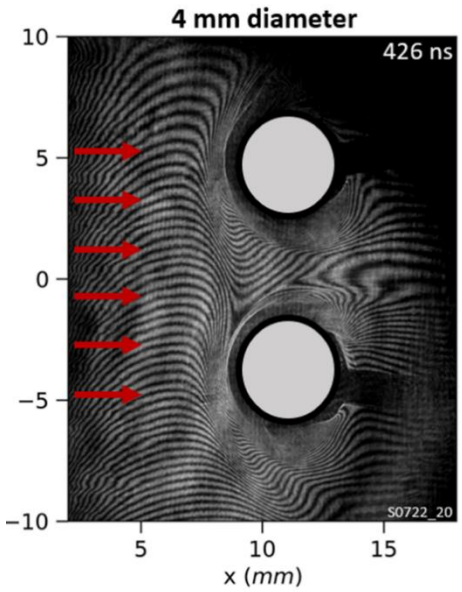

Fig. 9. Laser interferogram of two 4mm diameter 30mm long quartz cylinders in the plasma flow from an aluminum inverse array. The length of the cylinders were aligned with he expected azimuthal field from the array (into the page).

Measurements of electron density, velocity, T_e and T_i are presented below along a set of points midway between the targets (fig 10) and close to one of the cylinders (fig. 11).

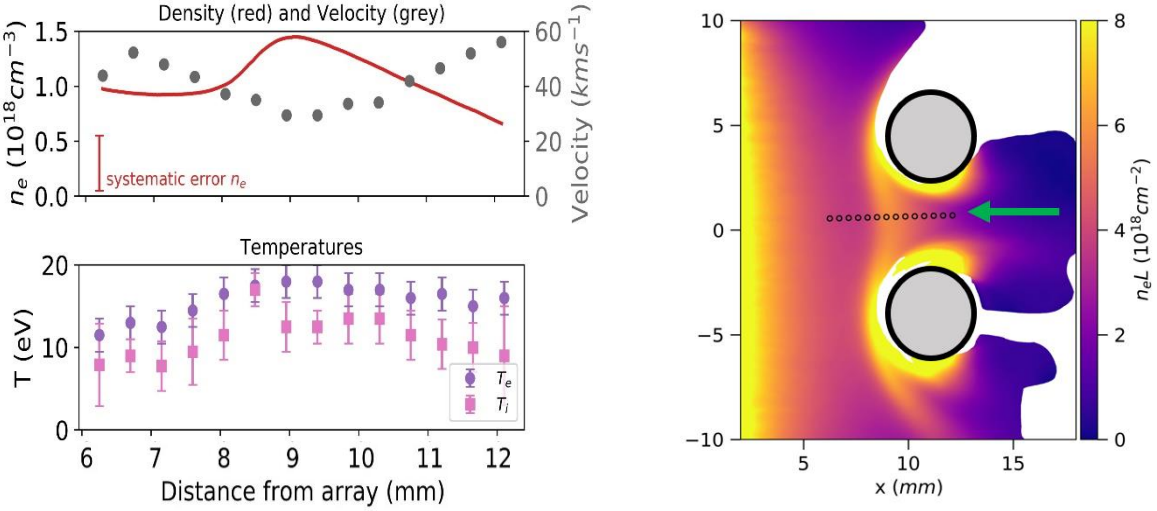

Fig. 10. Right: Electron line density map of plasma flow around two 4mm diameter quartz cylinders, also showing the 14 independent points of Thomson scattering along a line midways between the cylinders . Left Measurements of plasma velocity (in x direction), electron density, T_e and T_i from these points.

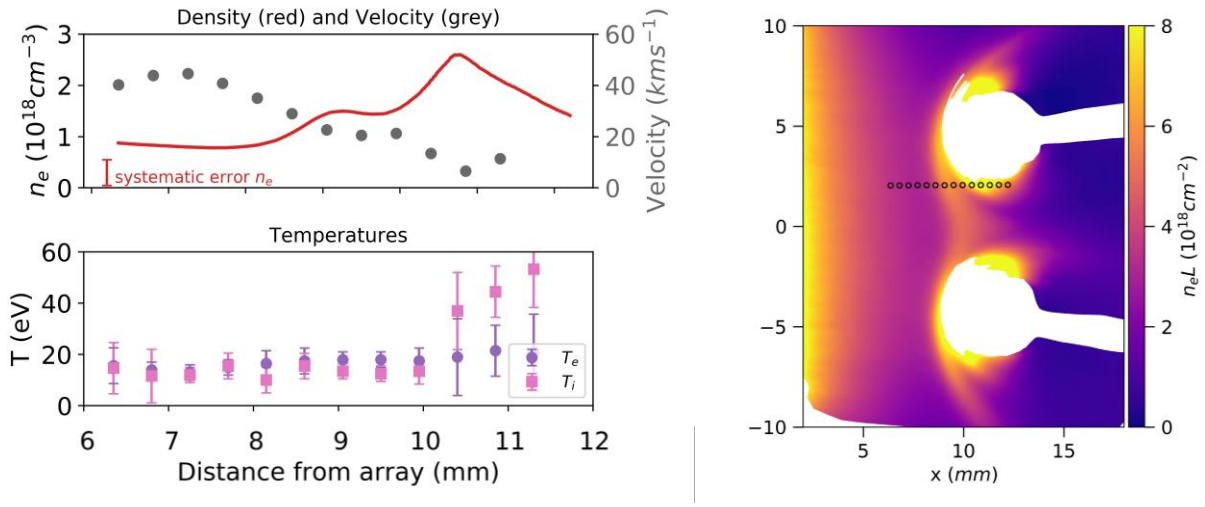

Fig. 11. Right: Electron line density map of plasma flow around two 4mm diameter quartz cylinders, also showing the 14 independent points of Thomson scattering along a line close to the upper cylinders surface . Left Measurements of plasma velocity (in x direction), electron density, T_e and T_i from these points.

As expected, measurements along a line close to the surface of a cylinder show a rapid increase in the ion temperature, as the probing points pass through the bow shock here; simultaneously the flow velocity drops and electron density increases. Measurements of the plasma in between the cylinders, meanwhile, indicate no strong shock wave in this region – the flow continues supersonically between the cylinders, and only gradual heating and changes to density and velocity are observed. Yet in this configuration we might have expected the formation of a Mach stem in between the cylinders as the shockwaves interacted together. This suggests that the presence of the magnetic field could also be affecting the formation of shock structures in the flow, again complicating the use of such magnetized plasma flows for purely hydrodynamics/hypersonics research.

To provide a large area of plasma flow without an entrained magnetic field, attempts were made to use a grid of copper wires to strip the field from the flow. Faraday imaging of 2 experiments with different grids is shown in fig. 12 below. With the grid wires placed 'horizontally' i.e. parallel to the magnetic field expected in the flow from the array, there was little effect on the rotation of the polarization of the laser beam as it passed through the plasma; however with the grid wires placed vertically, the angle of rotation was decreased by a factor of 4, indicating that with the majority of the magnetic field being removed from the flow. Subsequent tests with targets in the flow downstream from the grid showed a reduced distance between the bow shocks and the targets and a reduction in the angle of shockwave consistent with less embedded field being in the flow, but the field was not completely eliminated.

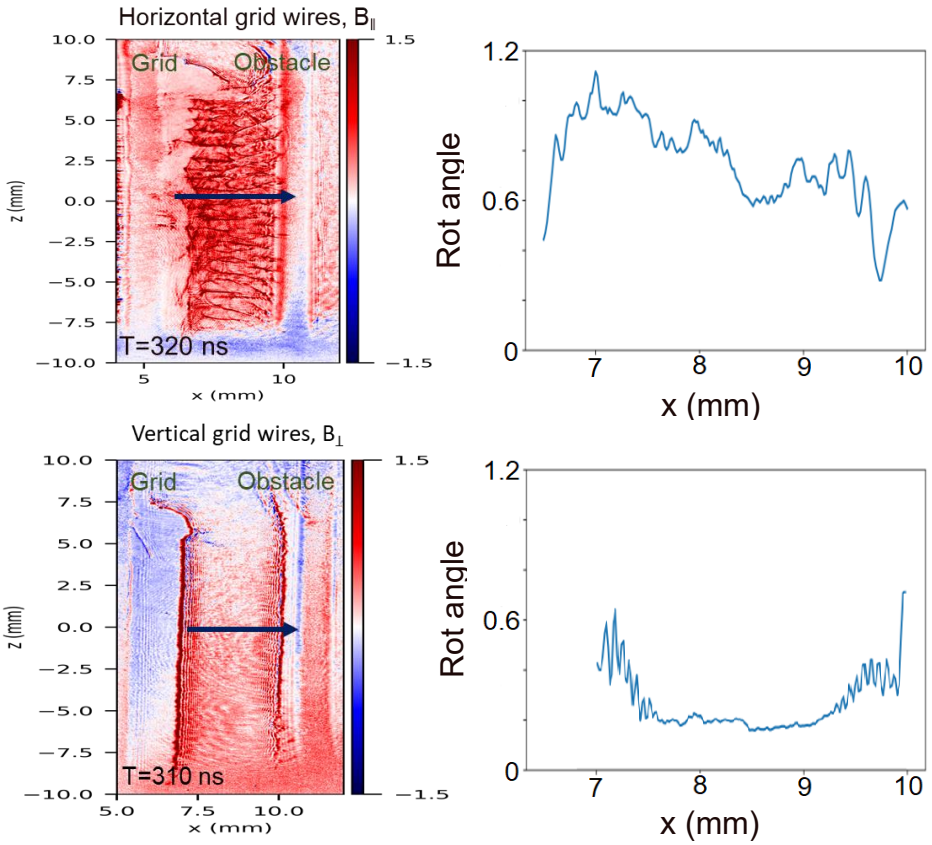

Fig. 12. Faraday probing images showing rotation of polarization of probing laser passing through the plasma flow from an inverse wire array with i) top – a grid of wires with wires placed parallel to the entrained field on the flow; ii) bottom – a grid of wires placed perpendicular to the entrained field in the flow.

4.2 Jets from radial foils

An XUV self emission image of the jet from a radial foil, along with an electron density map generated via interferometry are shown in fig. 13. These reveal a narrow, ~3-4mm diameter, collimated jet stretching for many cm above the cathode. Thomson scattering measurements demonstrated that the velocity of the jet was 50-100 kms^{-1} , slowing down as the experiment progresses, T_i / T_e in the jet was ~10eV and n_e~ $1x10^{19}$ cm^{-3}. These numbers suggest a sonic Mach number, M_s, 3-5 i.e. into the hypersonic regimes, providing no magnetic fields affect the flow of the jet.

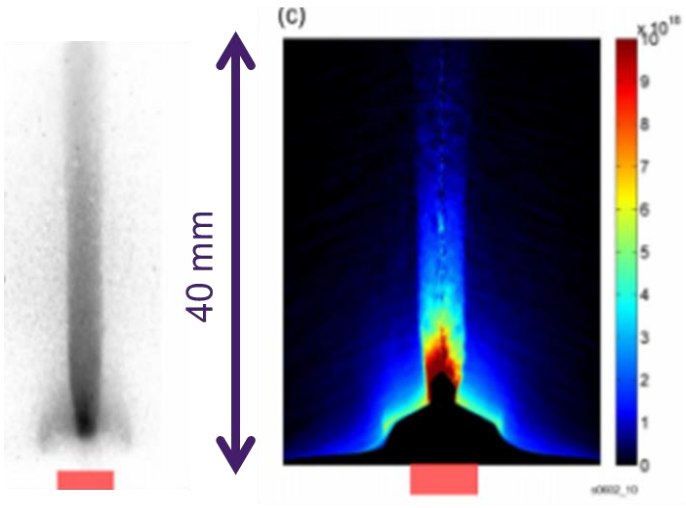

Fig. 13. Left: XUV self emission image of the jet from a radial foil experiment. Right: Electron density map interpreted from laser interferogram. Black represents an area that cannot be probed by the interferometry system.

Faraday rotation imaging, such as that show in fig. 14, indicates that the magnetic field inside the jets remains very small over the course of an experiment. Note that in fig. 14 a metal disk was placed above the radial foil, this acted to help test the Faraday rotation diagnostic, with ablated plasma from the foil (along with field) piling up against the disk.

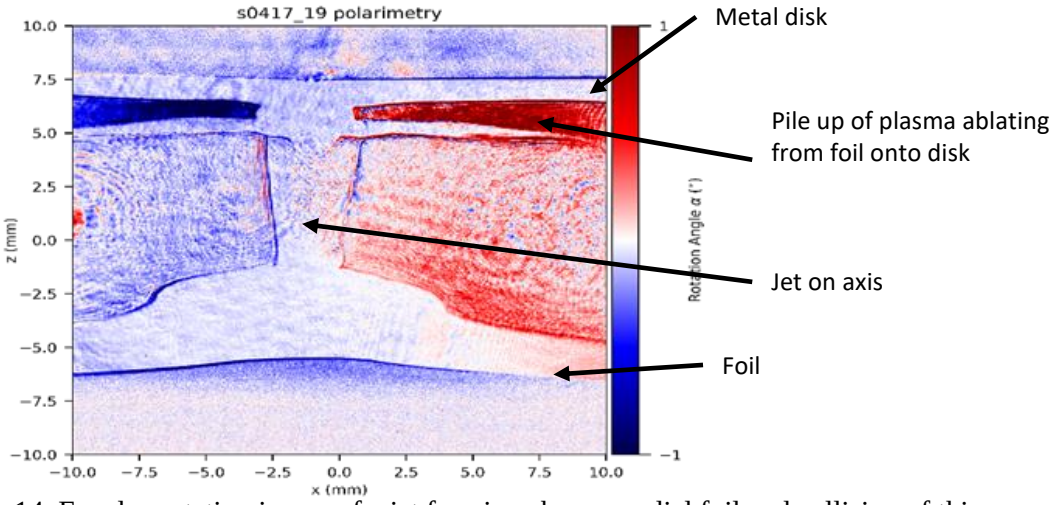

Fig. 14. Faraday rotation image of a jet forming above a radial foil and collision of this jet/ablated plasma from the foil with a metallic disk above the experiment.

The use of the jet as a dense plasma flow was then explored in a series of interaction experiments (with targets smaller than the jet diameter). A small sphere ~0.5mm in diameter was placed into the jet, resulting in the formation of a simple bow shock. This shock originated close to the surface of the target as would be expected for a purely hydrodynamical flow. The opening angle of the shock was however difficult to measure due to it colliding with the edge of the jet.

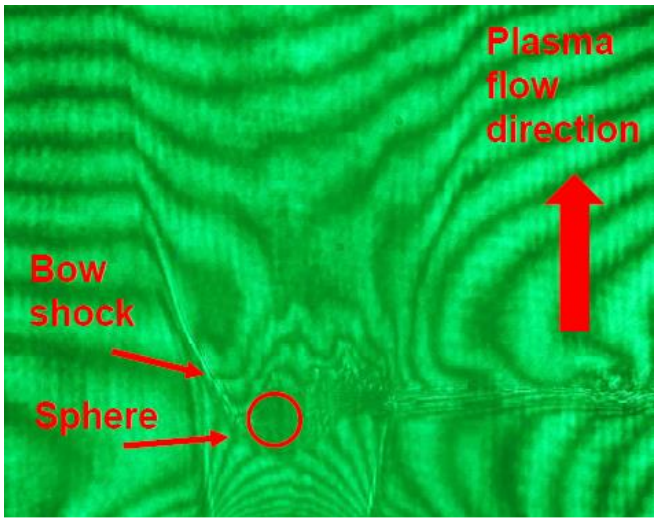

Fig. 15. Interferogram of small spherical target in plasma jet from radial foil

A small, 0.5mm, diameter rod suspended along the jet produced surprisingly complex interactions with the flow that evolved rapidly during the experiment. Initially a single bow shock originating from the end of the rod was observed in interferometry and laser shadowgraphy images, as shown in fig. 16. We note that shadowgraphy images are sensitive to the gradients of the refractive index, so highlight the presence of shocks and turbulence.

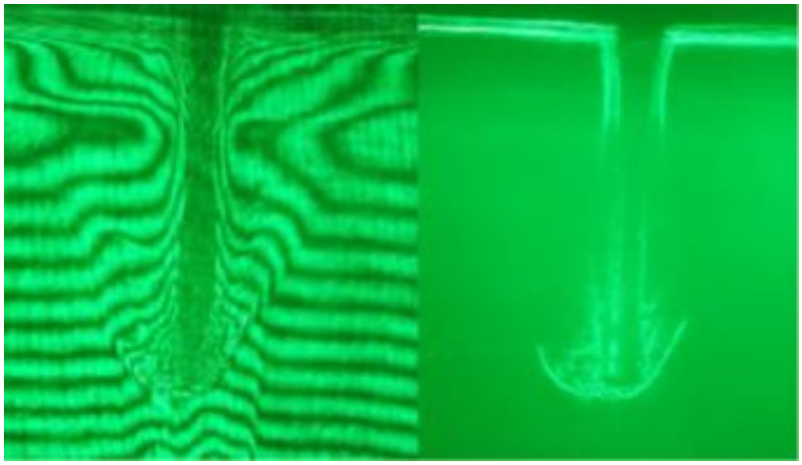

Fig. 16. 0.5mm rode suspended along direction of plasma flow in jet from radial foil. Left: Interferometry image. Right: shadowgraphy image.

Later in time this interaction develops into a series of "nested" shocks distributed along the rod, as shown in fig. 17. The cause for the multiple shock formation is currently unknown, and requires further studies. One possibility we consider is a radiative cooling instability developing in the bow shock - a fast reduction of the post-shock temperature due to radiative cooling could lead to shock oscillations, similar to discussed in the context of the temporal variability of astrophysical accretion shocks [8]. Other possible reasons for the formation of the multiple shocks include reflection and re-reflection of the original bow shock between the rod and edge of the jet, and the development of Kelvin-Helmholtz instability in the boundary layer at the rod surface.

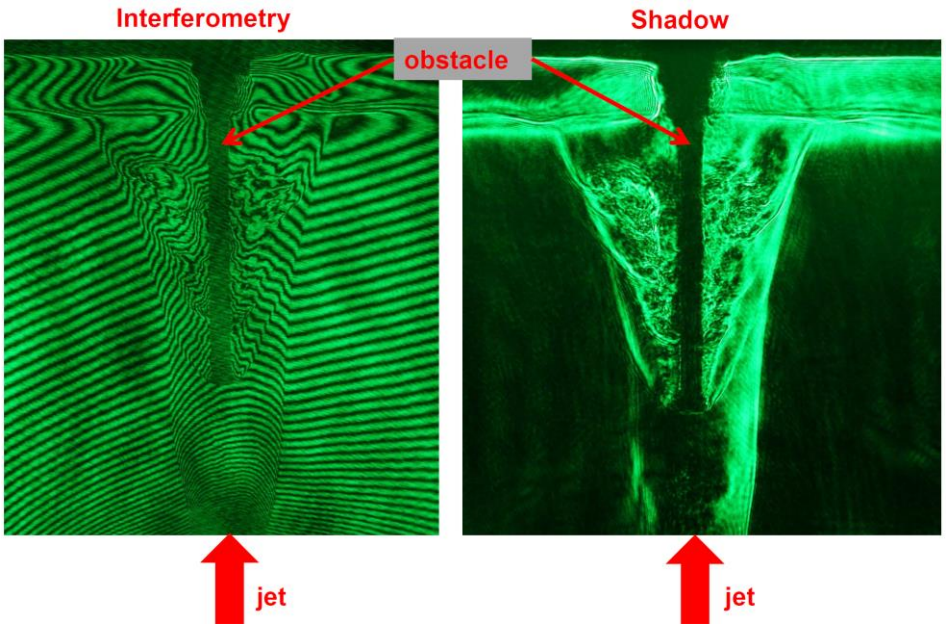

Fig. 17. Interaction of a supersonic jet propagating along a 0.5mm diameter rod positioned on the jet axis. Interaction leads to formation of several "nested" bow shocks along the rod length. Left- an interferogram and right is a shadowgram obtained in the same experiment. After interaction with the rod the jet collides with a planar obstacle.

4.3 Radiatively driven experiments

Whilst the use of jets from radial foils appears to produce unmagnetized plasma flows at hypersonic velocities, the small size of the jet limits the target size that can be utilized and – as we have observed – may produce complicated interactions far removed from the target. From this point of view the approach of using radiatively driven ablation seems more attractive – given the intensity of the soft X-ray source relatively large ablation targets can be used to produce wide plasma flows, allowing large targets for hydrodynamics experiments. Further it also removes a restriction on the plasma flow only being made from metal wires or foils. Using a radiative drive insulators or semi-conducting materials can all be utilized.

Preliminary experiments were carried out using a setup which is somewhat simpler than the one which is shown in Fig. 5 and 6 in order to characterize the conditions of radiatively driven plasma flows in the absence of a glass obstacle. These initial experiments were diagnosed with optical fast-frame imaging; laser interferometry; and Thomson scattering.

Data from the high speed optical emission camera indicated that the plasma flows which were launched by X-Ray irradiation did not cool or decelerate rapidly after the X-Ray pulse, with the flows maintaining for timescales >>100ns. The data also suggested that plasma flows were spatially uniform over length scales on the order of 1 cm. Interferometry allowed a quantitative measure of line integrated electron density to be obtained. It was found that characteristic values were on the order of $5 \times 10^{17} \mathrm{cm}^{-3}$. Thomson scattering provided measurements of plasma temperatures; velocities; and average degrees of ionization. It was found that $\mathrm{T_e} = \mathrm{T_i} \sim 10$ eV; $\mathrm{V_{flow}} \sim 6 \times 10^4\ \mathrm{ms}^{-1}$; and $Z \sim 6$.

Combining these results suggests an ion sound speed of $1.5 \times 10^4\ ms^{-1}$ and a sonic Mach number of $M_S \sim 4$. This value is well within the supersonic regime although it sits a little below the hypersonic threshold. In the future we could explore reducing the ion sound speed by increasing the average atomic mass of the plasma. It is likely that this would allow us to access conditions in which $M_s > 5$.

To build on these initial results, we performed some experiments in which an obstacle was placed in an ablated plasma flow, using the setup described in section 3.3. An interferogram from such an experiment is shown in fig. 18. In this image, the positions of the silicon target and glass obstacle are indicated. The location of the shade (designed to prevent the irradiation of the target by the driving X-Ray flux) is also shown. The X-Ray flux from the Z-pinch comes from the top right corner of the image.

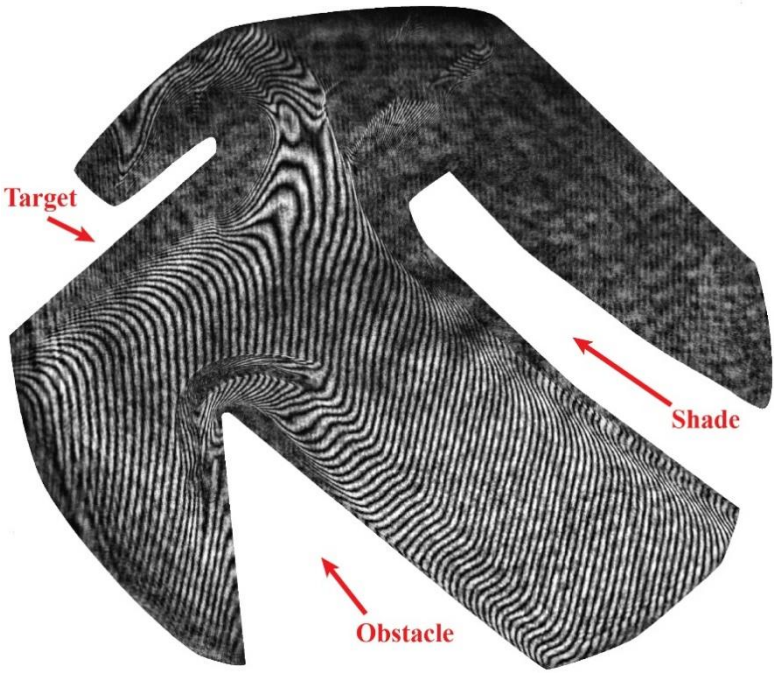

Fig.18 Laser interferometry data from a radiatively driven experiment with the positions of the silicon target, shade, and glass obstacle labeled.

The most obvious feature in this interferometry data is a wide bow shock, formed on the tip of the wedge-shaped glass obstacle. This is surprising: given the initial conditions of the experiment, we expected the formation of two oblique shocks launched off the two angled surfaces of the obstacle. The bow shock forms because there is significant ablation from the top-right surface of the glass obstacle (evidence of this can also be seen in the interferogram). The obstacle-ablation is likely due to the reradiation of X-Rays from hardware located near to the Z-Pinch, which was not fully blocked by the X-Ray shade. The ablated obstacle-material presented a blunt surface to the plasma flowing from the silicon and therefore the formation of a bow shock is consistent with hydrodynamic theory. In the future, the design of the target assembly can be adjusted to exclude this reradiation, preventing the ablation of material from the obstacle.

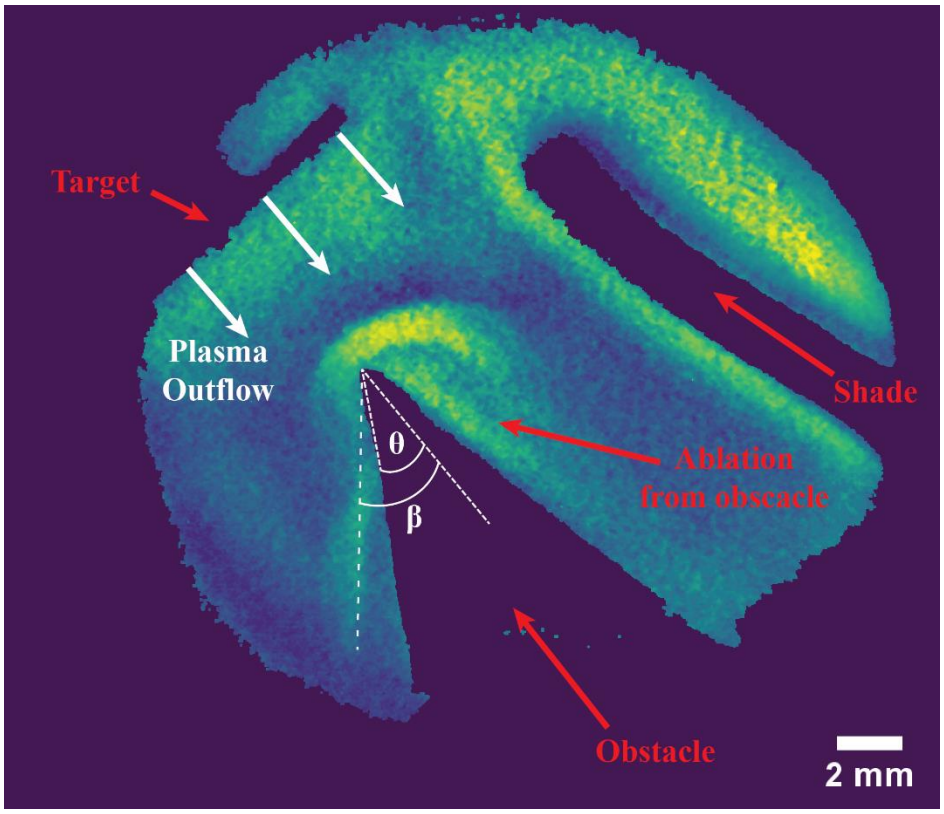

Fig.19 Optical self-emission data from an X-Ray driven experiment. The position of silicon target, glass obstacle, and X-Ray shade are shown. The angles θ and β, for the oblique shock launched from the lower side of the obstacle, are also indicated.

The lower-left side of the obstacle faces away from the pinch, so is more effectively shielded from reradiation, and does not ablate. In the interferometry data there is a subtle signature of (what could be) a shockwave launched from this surface. Unfortunately, the orientation of fringes in the interferogram mean that the diagnostic is not particularly sensitive to density changes in the direction perpendicular to this side of the obstacle. Fig. 19 shows a frame of optical self-emission data which was captured at the same time as the interferometry shown in the previous figure. The morphology of the feature launched from the lower side of the obstacle is much clearer here than in the in the interferometry. Furthermore, we see evidence of this feature from self-emission data spanning an interval of 100 ns. This suggests the feature is not transient but rather that it persists for many hydrodynamic timescales. If we interpret this region of enhanced self-emission as an oblique shock, then the data implies an opening angle of $\beta = 45 \pm 3\,°$. The annotations to the figure give an indication of how this was measured.

From the setup geometry we know that the angle between the obstacle and the initial flow direction was $\theta = 35\,°$. If we take $M_S = 4$ and $\gamma = 1.2$ (as was inferred from previous experiments), then the $\beta - \theta - M$ relation yields $\beta = 47\,°$. We therefore conclude that the morphology of the region of enhanced self-emission which we observe is consistent with the formation of an oblique shock as described by the standard hydrodynamic theory i.e. the flow

from plasma flow from the silicon ablator and its interaction with the obstacle were unaffected by magnetic field.

5.0 CONCLUSIONS

Several different experimental configurations were explored in order to create a pulsed power driven test bed for hypersonics research. Initially dense, supersonic plasma flows were created using inverse wire array z-pinches. The plasmas created typically had electron densities ~10^{18} cm^3, temperatures ~10eV and speeds of ~50kms^{-1}. This corresponded to a sonic Mach number in the flows of ~2.5 and the flows had the advantage creating large areas/volumes of plasma for interaction experiments. However magnetic fields entrained into the plasma flow at their creation reduced the effective Mach number, strongly affecting shock wave experiments – in particular magnetic field could pile up at a target, increasing the distance between the bow shock and the target and widening the shock wave. Attempts to strip the magnetic field from the plasma flow were made, but it proved difficult to remove its effects entirely. The plasma flow above a radial foil was then explored. This created a jet of plasma at higher density, n_e ~ 10^{19} cm^{-3}, with faster velocities, up to 100kms^{-1}, and with minimal entrained magnetic field – a purely hydrodynamic flow with a Mach number ~5. The small diameter of the jet, ~3mm, limited the size of targets that could be used in interaction experiments though such experiments did produce a series of interesting effects, in particular with nested shockwaves/turbulent effects being observed on the outside of rods placed parallel to the plasma flow. In a final set of experiments we utilized intense bursts of soft X-rays to ablate a target and create a plasma flow. The X-rays were created using pulsed power to drive an imploding wire array z-pinch, resulting in intensities ~ 10$GWcm^{-2}$ at the ablators surface. Outflows of plasma from the ablator were long lived, cm in scale, had electron densities ~10^{18} cm^{-3}, temperatures ~10eV and velocities ~60kms^{-1}. Experiments interacting the flow with a wedge target suggested the mach number of the flow was ~4, which agreed well with the calculated sonic mach number, confirming the flow was purely hydrodynamic.

Of the 3 experimental configurations explored in the project using radiation driven ablation of a target is the most promising for future hypersonics research. This configuration effectively separates the creation of plasma from the current (and associated magnetic field) of the pulsed power driver, instead relying on the driver to create high powers and yields of soft X-ray radiation. In these experiments the area of the ablator can readily be increased and its material changed. In particular increasing the Z of the target should reduce the ion sound speed in the flow of ablated plasma (from cooling) and allow us to access conditions in which $M_s > 5$.

The majority of tasks set out in the original project description have been accomplished. The main exception being the task to diagnose target material from interaction experiments being ablated into the flow. Now a more reliable system for creating highly supersonic/hypersonic flows has been created, this could be readily explored in future experiments using a new optical emission spectrometry system that has been recently developed at MAGPIE. Future research could also see the radiatively driven system used to investigate more complex hypersonic interactions – for instance two or more ablation targets could be placed to produce colliding flows. Fig. 20 shows an initial experiment in which 2 silicon ablators were placed at 90^0 to each other. The dense plasma outflow from each target collided with each other producing a high speed plasma jet.

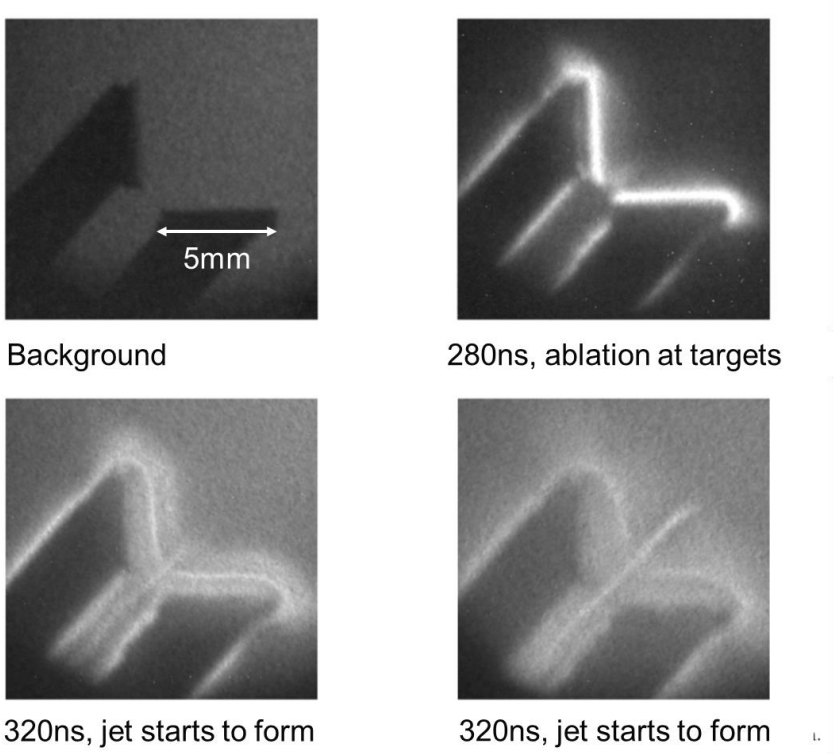

Fig.20 Series of optical self emission images from an experiment with 2 ablation targets angled towards each other. The dense, high speed plasma outflows from each target collided, forming a jet.

6.0 REFERENCES

[1] A. Harvey-Thompson, S. Lebedev, S. Bland, J. Chittenden, G. Hall, A. Marocchino, F. Suzuki-Vidal, S. P. J. Bott and C. Ning, "Quantitative analysis of plasma ablation using inverse wire array Z pinches," *Phys Plasmas,* p. 22701, 2009.

[2] I. Mitchell, J. Bayley, J. Chittenden, J. Worley, A. Dangor, M. Haines and P. Choi, "A high impedance mega-ampere generator for fiber z -pinch experiments," *Rec. Sci. Instrum,* p. 1533, 1996.

[3] G. Swadling, S. Lebedev, G. Hall, S. Patankar, N. Stewart, R. Smith, A. Harvey-Thompson, G. Burdiak, P. de Grouchy, J. Skidmore, L. Suttle, F. Suzuki-Vidal, S. Bland, K. Kwek, L. Pickworth, M. Bennett, J. Hare, W. Rozmus and J. Yuan, "Diagnosing collisions of magnetized, high energy density plasma flows using a combination of collective Thomson scattering, Faraday rotation, and interferometry," *Rev Sci Instrum,* p. 11E502, 2014.

[4] L. Suttle, J. Hare, J. Halliday, S. Merlin, D. Russell, E. Tubman, V. Valenzuela-Villaseca, W. Rozmus, C. Bruulsema and S. Lebedev, "Collective optical Thomson scattering in pulsed-power driven high energy density physics experiments," *Rev Sci Instrum,* p. 33542, 2021.

[5] S. Lebedev, A. Frank and D. Ryutov, "Exploring astrophysics-relevant magnetohydrodynamics with pulsed-power laboratory facilities," *Rev. Mod. Phys,* p. 025002, 2019.

[6] S. Lebedev, D. Ampleford, S. Bland, S. Bott, J. Chittenden, J. Goyer, C. Jennings, M. Haines, G. Hall, D. Hammer, J. Palmer, S. Pikuz, T. Shelkovenko and T. Christoudias, "Physics of wire array Z-pinch implosions: experiments at Imperial College," *Plasma Physics and Controlled Fusion,* 2005.

[7] D. Sinars, R. Lemke, M. Cuneo, S. Lebedev, E. Waisman, W. Stygar, B. Jones, M. Jones, E. Yu, J. Porter and D. Wenger, "Radiation Energetics of ICF-Relevant Wire-Array Z Pinches," *Phys Rev Lett,* p. 145002 , 2008.

[8] R. Sutherland, G. Bicknell and M. Dopita, "The Numerical Simulation of Radiative Shocks. II. Thermal Instabilities in Two-dimensional Models," *Astrophysical Journal,* p. 238, 2003.

APPENDIX A - Publications and Presentations

INVITED TALKS (2017-2021)

Invited talks that have used/leveraged research from the AFOSR funding:

Suttle, L. "Magnetic reconnection experiments on the Magpie pulsed power generator" - Invited seminar, University of Warwick Centre for Fusion, Space and Astrophysics (Online, Feb 2021)

Suttle, L. "Collective Thomson Scattering in pulsed power driven HEDP experiments on MAGPIE"– Invited Talk, 23rd Topical Conference on High-Temperature Plasma Diagnostics (Online, Dec 2020)

Suttle, L. " Interacting magnetized plasma flows in pulsed-power driven experiments" – Invited Talk, 46th EPS Conference on Plasma Physics (Milan, Italy 2019)

Suttle, L. Interactions of magnetized plasma flows in pulsed-power driven experiments – Invited Talk, 6th Workshop on Magnetic Fields in Laboratory High Energy Density Plasmas (Pingtang, China 2019)

Suttle, L. "Pulsed-power driven magnetic reconnection experiments" – Invited Talk, 12th International Conference on High Energy Density Laboratory Astrophysics (Kurashiki, Japan 2018)

CONTRIBUTED CONFERENCE PRESENTATIONS (2017-2021)

Contributed talks and posters that have used/leveraged research from the AFOSR funding:

Suttle, L. "Magnetized plasma flow interactions in pulsed power driven experiments" – Contributed Talk, 62nd Meeting of the APS Division of Plasma Physics (Online, 2020)

Suttle, L. "Magnetized shock experiments using exploding wire arrays" – Contributed Talk, 11th International Conference on Dense Z-Pinches (Beijing, China 2019)

Suttle, L. "The interaction of a magnetized plasma flow with strongly magnetized obstacles in HEDP experiments" – Contributed Talk, 60th Meeting of the APS Division of Plasma Physics (Portland OR, USA 2018)

Suttle, L. "Interaction of a magnetized plasma wind with strongly magnetized obstacles in HEDP experiments" – Poster Presentation, 12th International Conference on High Energy Density Laboratory Astrophysics (Kurashiki, Japan 2018)

Tubman, E.R., "Investigations of controlled, supersonic, magnetized plasma flows on the formation of bow shocks" - Talk, EPS 2018 (Prague, Check Rep)

Russell, D.R., “The effect of advected magnetic fields in jet propagation experiments” - Talk, EPS 2018 (Prague)

Russell, D.R. “Shock reflection in a magnetized, collisional laboratory plasma” - Contributed Talk, 62nd Meeting of the APS Division of Plasma Physics (Online, 2020)

Tubman, E. “Magnetically Collimated Plasma Jets From Radial Foil Z-Pinch” - Contributed Talk, 61st Meeting of the APS Division of Plasma Physics (Fort Lauderdale, FL, USA 2019)

Tubman, E. “Oblique shocks formed in magnetized plasma flows” - Contributed Talk, 60th Meeting of the APS Division of Plasma Physics (Portland OR, USA 2018)

Russell, D.R.. “The effect of advected magnetic fields in jet propagation experiments” - Contributed Talk, 60th Meeting of the APS Division of Plasma Physics (Portland OR, USA 2018)

Lebedev S.V. “Recent Magnetised High Energy Density Experiments on the MAGPIE Pulsed Power Generator” - Poster, 60th Meeting of the APS Division of Plasma Physics (Portland OR, USA 2018)

PUBLICATIONS

Upcoming publication:

D.R. Russell, “Bow shock interaction experiments in a magnetised collisional plasma” - PhD thesis, Imperial College London, 2021.

L. Suttle, J. Hare, J. Halliday, S. Merlin, D. Russell, E. Tubman, V. Valenzuela-Villaseca, W. Rozmus, C. Bruulsema and S. Lebedev, "Collective optical Thomson scattering in pulsed-power driven high energy density physics experiments," Rev Sci Instrum, p. 33542, 2021.

J.D. Hare, G.C. Burdiak, S. Merlini, J.P. Chittenden, T. Clayson, A.J. Crilly, J.W.D. Halliday, D.R. Russell, R.A. Smith, N. Stuart, L.G. Suttle and S.V. Lebedev, “An imaging refractometer for density fluctuation measurements in high energy density plasmas”, Rev. Sci. Instrum. **92**, 033521 (2021)

L.G. Suttle, G.C. Burdiak, C.L. Cheung, T. Clayson, J.W.D. Halliday, J.D. Hare, S. Rusli, D.R. Russell, E.R. Tubman, A. Ciardi, N.F. Loureiro, J. Li, A. Frank, and S. V Lebedev, “Interactions of magnetized plasma flows in pulsed-power driven experiments”, Plasma Phys. Control. Fusion **62**, 014020 (2020)

J.D. Hare, J. MacDonald, S.N. Bland, J. Dranczewski, J.W.D. Halliday, S. V. Lebedev, L.G. Suttle, E.R. Tubman, and W. Rozmus, “Two-colour interferometry and Thomson scattering measurements of a plasma gun”, Plasma Phys. Control. Fusion **61**, 085012 (2019)

J.D. Hare, L.G. Suttle, S. V. Lebedev, N.F. Loureiro, A. Ciardi, J.P. Chittenden, T. Clayson, S.J. Eardley, C. Garcia, J.W.D. Halliday, T. Robinson, R.A. Smith, N. Stuart, F. Suzuki-Vidal, and

E.R. Tubman, “An experimental platform for pulsed-power driven magnetic reconnection”, Phys. Plasmas **25**, 055703 (2018)